ELSEVIER

Catalysis Today 38 (1997) 235–242

CATALYSIS TODAY

Characteristics of Pt/H-beta and Pt/H-mordenite catalysts for the isomerization of *n*-hexane

Jeong-Kyu Lee, Hyun-Ku Rhee*

Department of Chemical Engineering, Seoul National University, Kwanak-ku, Seoul 151-742, South Korea

Abstract

Bifunctional Pt/H-beta and Pt/H-MOR catalysts were prepared under various pretreatment conditions and applied to the isomerization of *n*-hexane. Pt/H-beta gave rise to the higher yield of high octane dimethylbutanes than the commercial Pt/H-MOR. To explain this result, both the dispersion and distribution of Pt clusters in the zeolite channels were investigated. The acidity and the distribution of acid sites in both catalysts were also examined by using ammonia and pyridine as probe molecules. Pt/H-beta was found to be a potential catalyst for the isomerization of *n*-hexane because Pt clusters could be well dispersed to give proper balance between metallic centers and acid sites in H-beta zeolite although its acidity was low compared with H-MOR.

Keywords: Pt/H-beta; Pt/H-mordenite; Isomerization; n-Hexane; Acidity; Pyridine

1. Introduction

The demand for branched alkanes increases in the reformulated gasoline pools due to the environmental regulations such as elimination of lead alkyl additives and limitation in the content of olefins, benzene and total aromatics. The Pt/chlorinated-alumina has been commercially used in the industrial process for the isomerization of *n*-paraffins [1]. Pt/H-MOR has been recently considered as a new generation of commercial catalyst for C_5/C_6 paraffin isomerization [2]. More recently, some authors have reported that zeolite beta and mazzite would be potential acid catalysts for hydroisomerization of *n*-alkanes [3,4]. However, the characteristic features of and comparative studies between Pt/H-MOR and Pt/H-beta for alkane isomerization are not available yet. The activity of bifunctional Pt/zeolite catalyst is strongly influenced not only by the numbers of acidic and metallic centers but also by the distribution of these centers in zeolites [5]. The final location of the metal clusters as well as the metal dispersion in the zeolite depends on the calcination and reduction conditions and thereby exercises influence over the activity for the isomerization of *n*-alkanes.

The purpose of this study is to examine the changes in the distribution and dispersion of metal clusters in the zeolite channels with the pretreatment conditions and their effect on the isomerization of *n*-hexane. The acidic properties of H-MOR and H-beta are to be investigated by using ammonia and pyridine as probe molecules. Finally, the difference in activity between Pt/H-MOR and Pt/H-beta will be discussed in detail.

*Corresponding author. Fax: (82-2) 888-7295; e-mail: hkrhee@plaza.snu.ac.kr

0920-5861/97/$32.00
PII S0920-5861(97)00072-2

2. Experimental

2.1. Synthesis and preparation of catalysts

Zeolite beta was synthesized hydrothermally in the Teflon-lined autoclave from Na_2O–SiO_2–Al_2O_3–$(TEA)_2O$–H_2O system using tetraethylammonium hydroxide (TEAOH) as template [6,7]. NaMOR was obtained from a commercial sample (PQ Copr., SiO_2/Al_2O_3=13.0). The elemental composition of zeolite beta was analyzed for Si, Al and Na by atomic absorption and inductively coupled plasma method. The structure and crystallinity of zeolite beta were examined by X-ray diffraction (XRD) and mid-infrared spectroscopy [7]. The NH_3-form zeolite was prepared by ion-exchange of zeolites with 1 M NH_4Cl solution overnight at 80°C and this procedure was carried out three times. The NH_3-form zeolite was then transformed to the H-form zeolite by calcining in air at 540°C for five hours. Platinum loaded zeolites containing 0.5 and 2.0 wt% platinum, respectively, were prepared by both the ion-exchange and incipient wetness impregnation methods using $[Pt(NH_3)_4]Cl_2$ as precursor.

Platinum loaded catalysts were dried at 110°C overnight and then heated at a rate of 0.5°C/min in O_2 flow (1 l/min g cat) up to various calcination temperatures T_c (200, 300, 350, 400 and 500°C). The catalysts were maintained at each of these temperatures for 2 h and allowed to cool down to the room temperature in He flow. Reduction was then performed in H_2 flow (200 cm^3/min g cat) by raising the temperature at a rate of 2°C/min to 500°C and the temperature was held at 500°C for 1 h. Physicochemical properties of the catalysts examined in this study are summarized in Table 1.

2.2. Catalyst characterization

For temperature programmed desorption (TPD) analysis, the bed of H-form zeolite (0.1 g) was heated at 500°C in He flow for 1 h. Ammonia or pyridine was introduced in He flow into the bed after cooling the bed to 100°C or 200°C, respectively. The TPD was started by increasing the temperature at a rate of 15°C/min. Temperature programmed reduction (TPR) experiment was conducted for the Pt/H-MOR and Pt/H-beta catalysts calcined up to various temperatures. After calcination, the catalysts were cooled down to the room temperature in N_2 flow. A continuous flow of H_2 (6 vol%) in N_2 carrier was directed over the catalysts and the temperature was increased from the room temperature to 715°C at a rate of 10°C/min.

For FTIR study of CO adsorbed catalysts, self-supporting wafers of Pt/H-beta and Pt/H-MOR were pretreated in situ under the same operation conditions as mentioned above in a glass cell which was fitted with NaCl windows and high-vacuum stopcocks. Afterwards, the cell was evacuated to a pressure of approximately 10^{-2}–10^{-3} Torr and cooled down to the room temperature. Then, samples were exposed to CO at 20 Torr for 15 min. The spectrum was recorded after evacuation to the base pressure at room temperature and 100°C, respectively, for 15 min.

Table 1
Physicochemical properties and acidic properties of catalysts used in this study

Catalyst	Si/Al	BET results		NH_3-TPD (mmol/g cat)		Pyridine-TPD (μmol/g cat)		Pyridine IR (relative absorbance)	
		S_g (m^2/g cat)	V_p (cc/g cat)	LT-peak[a] (T_m,°C)	HT-peak[b] (T_m,°C)	LT-peak[c]	HT-peak[d]	PyL[e]	PyH^{+f}
H-MOR	6.5	501	0.209	0.63 (230)	0.48 (550)	12.72	10.50	3.22	1.00
H-Beta	15.4	698	0.234	0.44 (225)	0.29 (375)	19.15	33.03	0.46	1.49

[a]Ammonia desorbed at 100~325°C.
[b]Ammonia desorbed above 325°C.
[c]Pyridine desorbed at 200~400°C.
[d]Pyridine desorbed above 400°C.
[e]Pyridine adsorbed on Lewis acid sites.
[f]Pyridine adsorbed on Brönsted acid sites.

Hydrogen chemisorption was performed in a static vacuum volumetric apparatus at *RT* to investigate metal dispersion. Two isotherms were obtained to determine the total amount of adsorbed H_2 and the amount of weakly adsorbed H_2. The volume of strongly adsorbed H_2 was determined by subtracting the two isotherms and extrapolating the results to the zero pressure. The detailed procedures are described elsewhere [7].

2.3. Reaction experiment

The reaction experiment was conducted in a fixed-bed downflow reactor with H_2/*n*-hexane molar ratio of 6.0 under the atmospheric pressure. *n*-Hexane (purity >99.5%) was fed to the reactor in H_2 flow by a microfeeder. The product was analyzed by on-line GC with FID and the analysis column was made of stainless-steel tube packed with Chemipack C_{18}. The hydrogenation of benzene was also conducted at 100°C with H_2/benzene molar ratio of 9.8 and WHSV=29.3 h^{-1} under the atmospheric pressure.

3. Results and discussion

3.1. TPD using ammonia and pyridine

The results of TPD for both H-beta and H-MOR are summarized in Table 1. Intense low temperature peak appeared for both zeolites due to the weakly adsorbed ammonia on silanol groups. The area and the position of high-temperature desorption peak, related to desorption of ammonia from strong acid sites, turned out to be much higher over H-MOR than over H-beta. This implies that the acidity of H-MOR is much stronger than that of H-beta.

While ammonia (kinetic diameter approx. 3.57 Å) can have access to almost all the acid sites in the microporous zeolites, pyridine with kinetic diameter of about 5.85 Å may not approach to the acid sites situated in relatively small pores. The results of TPD using pyridine are also given in Table 1. The acidity determined by pyridine TPD conflicted with the "total acidity" probed by TPD using ammonia. As compiled in Table 1, the amount of desorbed pyridine was much larger over H-beta.

The results from in situ FTIR spectroscopy of pyridine adsorbed catalysts are presented in the last column of Table 1. The numbers in Table 1 indicate the relative absorbances of PyH^+ and PyL bands on H-MOR and H-beta zeolites. In accordance with the results from TPD using pyridine, the absorbance of PyH^+ on H-beta was higher than that on H-MOR although the amount of ammonia desorbed at high temperature was much higher over H-MOR. These conflicting results might be caused by the facts that H-beta can accommodate much more pyridine molecules than H-MOR because H-beta has larger pore volume than H-MOR and that pyridine cannot have access to some of the acid sites contained in H-MOR. Based on these results, one may deduce that there exist more acid sites, which could serve as adsorption sites for relatively large molecules such as mono- and di-branched isoalkenes, in H-beta compared with H-MOR.

3.2. TPR of catalysts

Presented in Fig. 1 are the TPR profiles obtained from Pt/H-MOR and Pt/H-beta calcined at various temperatures. The two major peaks at low and high temperatures are designated as α and β peaks, respectively. We notice from Fig. 1 that while the H_2 consumption remained nearly constant for Pt/H-MOR irrespective of T_c, it increased with T_c for Pt/H-beta. The large amount of H_2 consumption in Pt/H-MOR compared with Pt/H-beta calcined at temperatures below 500°C indicates that there were some PtO_2 species formed by autoreduction of $Pt(NH_3)_4^{2+}$ ions during oxidative deammination. For Pt/H-beta calcined at 500°C, the H_2 consumption was as high as that for Pt/H-MOR and this indicates the existence of Pt^{4+} species.

In contrast to the case of Pt/H-MOR, the α peaks were not detected from Pt/H-beta. Preferential sites for extraframework charge-balancing cations in H-MOR are the center of 8-MR and the wall of the main channel [8,9]. After ion-exchange, however, $Pt(NH_3)_4^{2+}$ cations were presumably located in the main channel rather than in the side pockets of 8-MR because the cations would not be allowed to diffuse into the side pockets due to their size. Once the cations were completely decomposed to Pt^{2+} ions, the ions would be located both in the main channels and in the

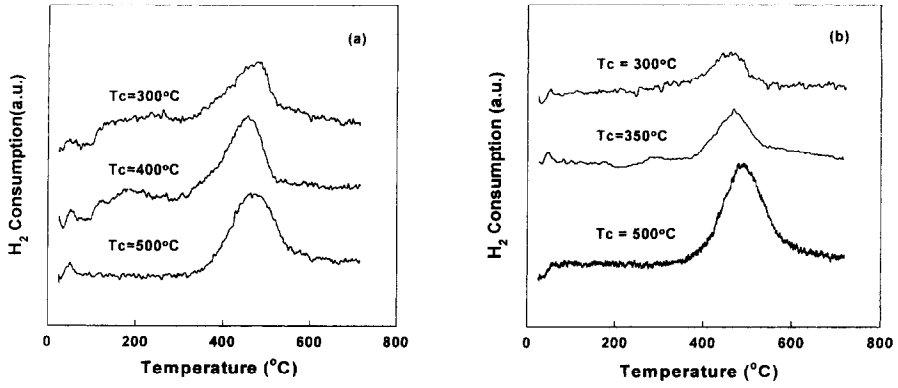

Fig. 1. TPR profiles from (a) Pt/H-MOR and (b) Pt/H-beta, respectively, calcined at various temperatures.

side pockets. Accordingly, the two TPR peaks above 100°C could be attributed to the reduction of Pt^{2+} ions located in the main channels of 12-MR and those at some hidden sites including the sites in the side-pockets. The area of α peak decreased with T_c and α peak disappeared when Pt/H-MOR was calcined at 500°C. In addition, the temperature for complete reduction shifted to the higher temperature range. These results suggest that as T_c was increased, the Pt^{2+} ions initially located in the wall of the main channels might have slowly migrated into the side pockets, in which Pt^{2+} ions could form more stable coordination with the zeolite.

3.3. *FTIR spectroscopy of CO-adsorbed catalysts*

The infrared spectra of CO adsorbed on Pt/H-MOR are presented in Fig. 2. At saturation coverage, three bands were observed at 2124, 2087 and 1867 cm^{-1}, respectively. The intense peak at 2087 cm^{-1} was assigned to the linear CO band and the small band at 1867 cm^{-1} to the bridging CO band. Since the absorbance ratio of bridging CO band to linear CO band was very low (0.04–0.07), Pt must have been highly dispersed in zeolites. As shown in Fig. 2, the absorbance of the band at 2124 cm^{-1} increased with T_c. The peak location suggests that this platinum species was in a low positive oxidation state. Kustov et al. [10] and Lamb et al. [11] assigned this peak to CO adsorbed on very small clusters or monoatomic Pt^I monocarbonyl species.

The peak position of linear CO band shifted to the lower wave number by 10 cm^{-1} when the sample was

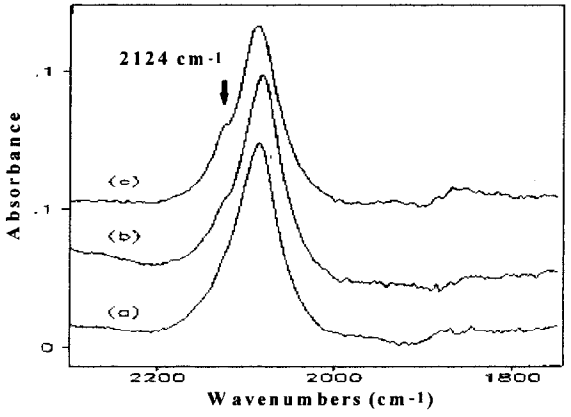

Fig. 2. Infrared spectra of CO from Pt/H-MOR catalysts calcined at various temperatures: (a) T_c=300°C, (b) T_c=350°C and (c) T_c=500°C.

evacuated at 100°C instead of at *RT*. The peak position of band at 2124 cm^{-1}, however, was unaffected by CO coverage. This indicates that CO species observed at 2124 cm^{-1} had little interaction with neighboring CO and the clusters serving as adsorption sites for CO were associated with isolated Pt species in H-MOR channel. Mortier [9] determined Ca^{2+} ion sites in CaMOR to show that the sites deepest in the side-pockets of 8-MR are preferentially occupied and the sites in the main channel of 12-MR were the second in population and stability of the cations at high temperature above 350°C. Mortier suggested that the favorable coordination of bipositive ions with oxygen ions would be the reason for the stability of Ca^{2+} ions in the side-pockets.

Table 2
H_{irr}/Pt values and activities for the isomerization of *n*-hexane and hydrogenation of benzene of Pt/H-MOR and Pt/H-beta catalysts calcined at different temperatures

T_c (°C)	Pt/H-MOR			Pt/H-beta		
	H_{irr}/Pt[a]	A_1[b]	TOF[c]	H_{irr}/Pt[a]	A_1[b]	TOF[c]
200	—	—	—	1.14	11.3	33.5
300	1.14	7.5	2.7	1.51	13.1	45.6
350	1.33	8.2	2.4	1.25	12.8	—
400	1.20	4.2	0.9	0.99	8.9	99.7
500	0.94	5.0	0.4	0.87	5.9	38.9

All catalysts contained 0.5 wt% Pt and were reduced at 500°C for 1 h.
[a]Determined by H_2 chemisorption.
[b]Activity for isomerization of *n*-hexane (μmol/s g cat).
[c]Turnover frequency for hydrogenation of benzene (molecules/s surface Pt atom).

Hence, the increase in absorbance of band at 2124 cm^{-1} with T_c may be regarded as another evidence that Pt^{2+} ions initially located in the main channel might have migrated into the side-pockets. After the reduction step, some of Pt clusters still remain in the side-pockets, where Pt clusters interact with H^+ to have electron deficient character. Therefore, it is reasonable to assign the band at 2124 cm^{-1} to CO adsorbed on isolated Pt clusters in the side-pockets of mordenite channel.

3.4. H_2 chemisorption

The H_{irr}/Pt values for Pt/H-MOR and Pt/H-beta calcined at various temperatures are given in Table 2. The maximum values of H_{irr}/Pt were obtained from Pt/H-MOR and Pt/H-beta calcined at 350°C and 300°C, respectively. The H_{irr}/Pt values of all the samples calcined at temperatures below 400°C were higher than the assumed stoichiometric value of 1.0. Independent EXAFS study of samples containing 2.0 wt% of platinum revealed that the nearest neighbor coordination numbers (CN) of platinum clusters were in the range of 5.7–9.5 depending on the pretreatment conditions. These CN values correspond to average diameters in the range of 8–15 Å. Since the growth of particles would be accelerated by the amount of metal loading [12], the average diameter of Pt particles in Pt/H-MOR and Pt/H-beta loaded with 0.5 wt% Pt is expected to be smaller than that in catalysts loaded with 2.0 wt% Pt. This result indicates that platinum clusters were well dispersed in the channels of both zeolites.

3.5. Comparison of the catalytic activity between Pt/H-MOR and Pt/H-beta

The composition of reaction products over Pt/H-MOR and Pt/H-beta are given in Table 3. For both catalysts, the highest yield of *i*-hexane was obtained at 280°C. The catalytic activity of Pt/H-beta was higher than that of Pt/H-MOR despite the higher acidity of the latter catalyst. It is to be noticed that the difference in activity between the two catalysts resulted in the difference in the yield of DMBs. The yield of methylpentanes (MPs) was nearly the same over both catalysts but the yield of DMBs was much higher over Pt/H-beta than over Pt/H-MOR.

The selectivity to DMBs at 270°C is plotted against the contact time in Fig. 3. At low contact time (or conversion), the selectivity to DMBs over Pt/H-MOR was higher than that over Pt/H-beta. As the contact

Table 3
Steady state product distributions from isomerization of *n*-hexane over Pt/H-MOR and Pt/H-beta catalysts

Catalysts	T (°C)	Conversion (%)	Product composition (wt%)				Σi-C_6	i-C_6 Selectivity (%)
			C_1–C_5	2-MP[a]	3-MP[b]	ΣDMB[c]		
Pt/H-MOR	270	70.7	1.2	33.8	21.8	13.9	69.5	98.3
	280	74.3	4.7	33.2	22.6	15.0	70.8	95.3
Pt/H-beta	270	78.4	1.2	34.8	22.6	19.7	77.1	98.4
	280	82.0	3.2	33.3	21.7	23.7	78.7	97.1

Reaction conditions: H_2/*n*-hexane=6.0, WHSV=1.58 h^{-1}, Total pressure=1 atm.
[a]2-methylpentane.
[b]3-methylpentane.
[c]2,3-dimethylbutane+2,2-dimethylbutane.

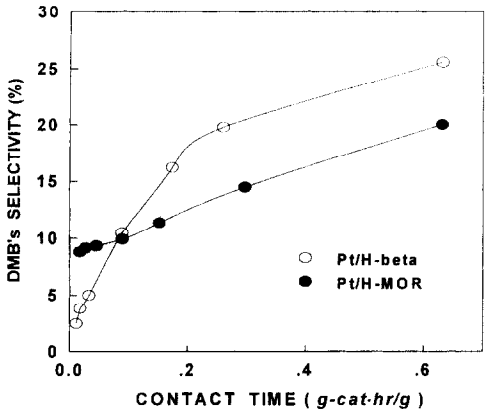

Fig. 3. Selectivity to DMBs as a function of the contact time over Pt/H-beta and Pt/H-MOR catalysts at 270°C (H_2/*n*-hexane=6.0).

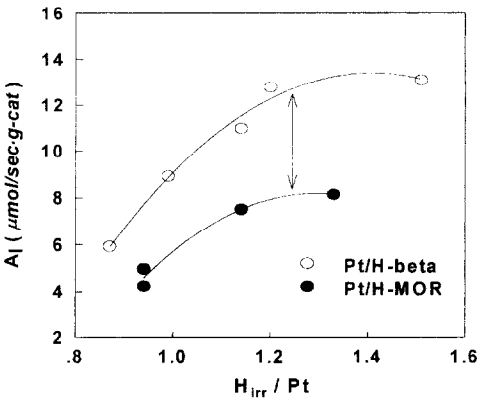

Fig. 4. Activity (A_I) for the isomerization of *n*-hexane as a function of H_{irr}/Pt over Pt/H-MOR and Pt/H-beta catalysts.

time increases, however, the selectivity was reversed between the two catalysts. The reversion of DMBs selectivity may be attributed to the combined effect of acidity, channel structure including pore size and dispersion as well as distribution of metallic centers. At low contact time, the rate of formation of DMBs from MPs was higher over Pt/H-MOR because the acidity of H-MOR was much higher than that of H-beta. At high contact time, the residence time of carbenium ions on acid sites would become much larger, and thus the structural effect and metal function in zeolite channels appear to play important roles in the formation of DMBs.

3.6. *Effect of thermal activation*

The Pt/H-MOR and Pt/H-beta catalysts were pretreated at various calcination and reduction temperatures to examine the effect of thermal activation on the isomerization of *n*-hexane. The catalytic activity for the isomerization of *n*-hexane is presented in Table 2. The highest activity was obtained for both catalysts calcined at 300–350°C and subsequently reduced at 500°C. When T_c was increased, the activity decreased rapidly.

If the acidities of both Pt/H-MOR and Pt/H-beta are unaffected by the thermal activation conditions adopted in this study, the activity variation may be ascribed to the change in metallic centers. The activities of Pt/H-MOR and Pt/H-beta are plotted against H_{irr}/Pt value in Fig. 4. When the H_{irr}/Pt value was low, the activity increased almost linearly with H_{irr}/Pt and then approached to a limiting value as H_{irr}/Pt increased. The ratios of metal sites to strong acid sites in the range of H_{irr}/Pt showing constant activity in Fig. 4 corresponded to 0.4 and 0.7 for Pt/H-MOR and Pt/H-beta, respectively. These values were higher than the ratio that was suggested as the critical ratio by Guisnet et al. [13] for the optimum performance with respect to *n*-heptane isomerization.

For identical value of H_{irr}/Pt, the activity of Pt/H-beta was higher than that of Pt/H-MOR and the difference in activity became larger as H_{irr}/Pt increased. The isomerization of *n*-hexane is believed to take place via bifunctional mechanism [14], involving both acid and metal sites. When metal loading is low, the activity increases proportionally to the hydrogenation function. If the metal component is present in sufficient excess to establish equilibrium between paraffin and associated olefin the activity is then governed by the acid function. The equilibrium was found to be established by loading 0.2–0.5 wt% of Pt in the previous study of Leu et al. [3] and Degnan et al. [15]. This was also confirmed by our experimental result. For identical value of H_{irr}/Pt, the activity of Pt/H-beta was higher than that of Pt/H-MOR and difference in the activity became larger as H_{irr}/Pt increased. If the number of metal sites are identical, the distribution of Pt clusters in zeolite channels would be responsible for the difference in activity.

To compare the hydrogenation activity between Pt/H-MOR and Pt/H-beta, the hydrogenation of benzene was conducted. If most of the Pt clusters were located on the outer surface of the zeolite crystallites, Pt/H-

MOR and Pt/H-beta catalysts would not have shown such a large difference in the hydrogenation activity. The hydrogenation activity of Pt/H-beta, however, was extremely high in comparison to that of Pt/H-MOR when the Pt dispersion was about the same for both catalysts as shown in Table 2. Therefore, the large difference in hydrogenation activity between the two catalysts might be attributed to the difference in the number of Pt clusters exposed to benzene or the accessibility of benzene to the Pt clusters in the zeolite channels.

According to the TPR and in situ CO-IR results, some of Pt clusters remained isolated in the side-pockets of H-MOR and these metallic centers may not serve as dehydrogenation/hydrogenation sites during the isomerization of *n*-hexane. In such a case, the metal/acid ratio in the main channel of H-MOR will decrease, so the selectivity to DMBs should be low at high conversion level over Pt/H-MOR as shown in Fig. 3.

In addition to the detrimental loss of metallic centers, mordenite has one-dimensional pore structure with side-pockets at the wall of main channels, so if the platinum clusters in the main channel grow in size to fit the pore size of H-MOR during the reduction step, many of acid sites as well as platinum clusters located in the interior to the pore-plugging large clusters near the pore mouth would become inaccessible to the reactant and reaction intermediates. On the other hand, zeolite beta consists of intergrowth of linear channels (5.7×7.5 Å) of 12-MR and tortuous channels (6.5×5.6 Å) with channel intersections. Therefore, even if one of the channels are blocked by large particles (the linear channel might be blocked first), reactant and reaction intermediates might have access to some of metal sites through the other channels. In conclusion, there are much more platinum sites that are accessible to benzene in Pt/H-beta and the diffusion of benzene to metal sites in Pt/H-beta would be much easier than in Pt/H-MOR.

4. Conclusions

The bifunctional Pt/H-MOR and Pt/H-beta were prepared and their characteristics for the isomerization of *n*-hexane were elucidated. Both the catalytic activity and the selectivity to high octane DMBs were higher over Pt/H-beta than over the commercial Pt/H-MOR. However, the selectivity was found dependent upon the conversion of *n*-hexane. The catalyst calcined at 350°C and subsequently reduced at 500°C gave rise to the highest metal dispersion and the best activity.

Although the "total acidity" probed by ammonia was higher over H-MOR, the "effective acidity" probed by pyridine was much higher over H-beta. For both Pt/H-MOR and Pt/H-beta, Pt clusters were found not only highly dispersed but also well distributed within the zeolite channels. For Pt/H-MOR, however, some of Pt clustes were isolated in the side-pockets of 8-MR and these metallic centers increased in population with the calcination temperature. In addition, pore blockage of H-MOR channels by large Pt clusters could have made some of the Pt sites inaccessible to reactant and reaction intermediates. Due to these effects, the hydrogenation activity of Pt/H-beta was observed much higher than that of Pt/H-MOR when the dispersion was identical for both catalysts.

In conclusion, the yield of DMBs over Pt/H-beta was higher than that over Pt/H-MOR because there were more acid sites accessible to bulky reaction intermediates such as methylpentenes and dimethylbutenes and Pt clusters were well dispersed in such way that the metallic centers might be balanced with acid sites in Pt/H-beta.

Acknowledgements

The financial support of Yukong Ltd. for this work was gratefully acknowledged.

References

[1] I.E. Maxwell and W.H.J. Stork, Stud. Surf. Sci. Catal., 58 (1990) 571.

[2] P.J. Kuchar, J.C. Bricker, M.E. Reno and R.S. Haizmann, Fuel Proc. Technology, 35 (1993) 183.

[3] L.-J. Leu, L.-Y. Hou, B.-C. Kang, C. Li, S.-T. Wu and J.-C. Wu, Appl. Catal., 69 (1991) 49.

[4] F. Fajula, M. Boulet, B. Cop, V. Rajacfanova, F. Figueras, T. Des Courieres, in: L. Guczi, F. Solymosi, P. Telenyi (Eds.), Proceedings of the 10th International Congress on Catalysis Budapest, Elsevier, Amsterdam, 1993, p. 1007.

[5] M. Guisnet, G. Perot, in: F.R. Ribeiro et al. (Eds.), Zeolite, Science and Technology, Martinus Nijhoff, Den Haag, 1984, p. 397.
[6] R.L. Wadlinger, G.T. Kerr, E.J. Rosinski, US Patent 3 308 069 (1967).
[7] J.K. Lee, H.T. Lee and H.K. Rhee, React. Kinet. Catal. Lett., 57 (1996) 323.
[8] S. Bordiga, C. Lamberti, F. Geobaldo and A. Zecchina, Langmuir, 11 (1995) 527.
[9] W.J. Mortier, J. Phys. Chem., 81 (1977) 1334.
[10] L.M. Kustov and W.M.H. Sachtler, J. Mol. Catal., 71 (1992) 233.
[11] M.M. Otten, M.J. Clayton and H.H. Lamb, J. Catal., 149 (1994) 211.
[12] S.T. Homeyer and W.M.H. Sachtler, J. Catal., 118 (1989) 266.
[13] V.L. Zholobenko, M.A. Makarova and J. Dwyer, J. Phys. Chem., 97 (1993) 5962.
[14] M. Maache, A. Janin, J.C. Lavalley and E. Benazzi, Zeolites, 15 (1995) 507.
[15] T.F. Degnan and C.R. Kennedy, AIChE J., 39 (1993) 607.